DETECTION AND LOCATION OF THE DEAD SEA SHOTS USING ADVANCED PROCESSING TECHNIQUES.

Vladimir Pinsky, Avi Shapira, Yefim Gitterman and Alona Malitzky

Geophysical Institute of Israel

Sponsored by The Defense Threat Reduction Agency

Contract No.DSWA01-97-C-0151

ABSTRACT

Seismic data of the Dead Sea calibration experiment, which provided Ground Truth source parameters, were used in studying advanced signal processing methods. The data set includes recordings of the SP stations of the Israel Seismic Network (ISN), the EILAT Experimental Seismic Array (EILESA) and the IMS primary station GERESS. There were no detection problems at ISN and Cypriot stations (r<500 km), equipped by the simplest STA/LTA algorithm. Meanwhile, low SNR at the GERESS (R=2400 km) did not allow to detect even the largest explosion by the routine automatic procedure.

We applied Adaptive Optimal Group Filter (AOGF) (Kushnir, 1995) method to the GERESS recordings, containing the explosion signal. The algorithm is based on computation of the preceding noise spectral matrix and theoretically provides undisturbed output signal with maximum SNR. The tool facilitated event detection, and yielded accurate estimations of the apparent velocity (±1 km/sec) and back azimuth ($\pm 2^0$). Equivalent results were obtained by the Maximum Likelihood Technique (MLT) (Bohme, 1995) – the highly sensitive moving window spectral analyzer of array data, destined mainly for the detection of multiple signals.

The same techniques were applied to the recordings of the EILESA – 8 station short period micro-array temporally deployed in the vicinity of the IMS BB station EIL. The algorithms provided satisfactory azimuth and velocity determination in spite of the poor array configuration. However, the estimates exhibited significant temporal variations of azimuth and apparent velocity attributed to heterogeneity of the upper crust.

Using ISN and CSN manual P picks for the three calibration explosions the best-fit 4 layer stratified model was evaluated for 500 km distance range, providing residual RMS = 0.2 sec The scatter of residuals didn't reveal systematic azimuth dependency. Then we applied robust automatic locator (Pinsky, 1999), developed in the frame of the contract, to the ISN recordings of the three events. The locator is the two stage procedure, using envelope location at the first stage to estimate the time intervals for the P, S first arrivals to the network stations. The second stage comprises automatic picking of the P, S first arrivals with robust fitting of the picks (eliminating outliers) to the travel time model. The results of the automatic location appeared close to the real epicenter and for the case of the best-fit model even better than the analyst solution, based on the conventional local model.

Key Words: Dead Sea explosions, automatic detection, location, parameter estimation, travel time.

OBJECTIVE

The major tasks of the CTBT monitoring are detection and location of seismic sources. Calibration explosions, such as the three detonated in the Dead Sea, serve the task providing travel time and azimuth corrections for tuning the IMS and other seismic networks and testing the assigned software. The main objective of this work was analysis of the waveforms from the Dead Sea calibration explosions at different recording systems and investigation of the travel times and behavior of several sophisticated algorithms for detection, location and parameter estimation using these recordings.

RESEARCH ACCOMPLISHED

1. Application of the Adaptive Optimal Group Filer (AOGF).

The main source parameters of the three Dead Sea explosions are presented in the Table 1. Signals of all the explosions were recorded with good SNR by all the stations within 500 km from the source: the Israel Seismic Network, Cyprus and Jordan seismic networks, CNF stations, BB IMS stations EIL and MRNI, so that there were no detection problems even for the simplest STA/LTA algorithm. The largest 5 t explosion was detected at GERESS (2400 km) as a weak signal, extracted though after careful pre-filtering. However, for many stations and arrays at R > 800 km (for example BRAR, Turkey) the signal is impossible to extract. This indicates practical distance and region limits for detection the explosive source of $m_b = 4$ from the Dead Sea area.

Table 1. Main parameters of the Dead Sea explosions.

Date	Origin time (O.T.), GMT	Coordinates	Total charge, t	Comments
8.11.99	13:00:00.33	31.5330N 35.4406E	0.5	Measurement accuracy: coordinates – 50 m, origin time – 5 msec
10.11.99	13:59:58.21	31.5338N 35.4400E	2.06	
11.11.99	15:00:00.795	31.5336N 35.4413E	5	

Main power of the signal is concentrated between 0.8 and 1.5 Hz, that doesn't change much with distance and provides good SNR at GERESS in this frequency band. Therefore, using this frequency band or close to it for GERESS recordings it was possible to estimate rather accurately azimuth and apparent velocity (the true Az=128.5 °, Vel.=12.15 km/sec), using usual wideband F-K analysis technique. Fig. 1. illustrates the estimates (we used for the analysis Kushnir & Haikin SNDA package) as maximum of the statistic at Az=132.5 °, Vel.= 12.32 km/sec for 0.8-1.8 Hz and Az=128.3 °, Vel.= 15.46 km/sec for 1.1-1.4 Hz frequency band respectively. We applied Adaptive Optimal Group Filter (AOGF) method (Kushnir, 1995) to the GERESS recordings, containing the explosion signal. The algorithm is based on computation of vector $\boldsymbol{R(f)}$ at each frequency *f:*

$$R^*(f)\,) = [H^*(f)\,F^{-1}(f)\,H(f))]^{-1}\,H^*(f)\,F^{-1}(f), \qquad (1)$$

where $\boldsymbol{H(f)}$ is a vector of the array response with element $h_n(f) = \exp(-2\pi i f \tau_n\,),\ n=1,\ldots,N$, $\boldsymbol{F(f)}$ is a matrix spectral density of the array noise. In the algorithm the $\boldsymbol{F(f)}$ matrix is estimated from the noise, preceding the signal.

The algorithm theoretically provides undisturbed output signal with maximum SNR for the true staring azimuth and apparent velocity. This property of AOGF is used in the SNDA (Seismic Network Data Analysis) package (Kushnir, Haikin, 1996) for Adaptive F-K analysis (AF-K). The AF-K (Fig. 2) results in Az=126.9°, Vel.=10.0 km/sec in the frequency band (0.8-1.5 Hz). In all cases the time interval used for the analyses was equal 5 sec.

For the signal extraction we applied SNDA version of the AOGF to the GERESS 25 channels recordings with staring azimuth Az=123.8° and apparent velocity Vel.=12.3 km/sec, filtered in the 1-3 Hz interval. The results of the AOGF and BEAM are shown on Fig.3 together with traces of the GERESS channel GED9 (with the best SNR). From the Fig. 3 we see that the AOGF has a slight advantage over the BEAM here.

a

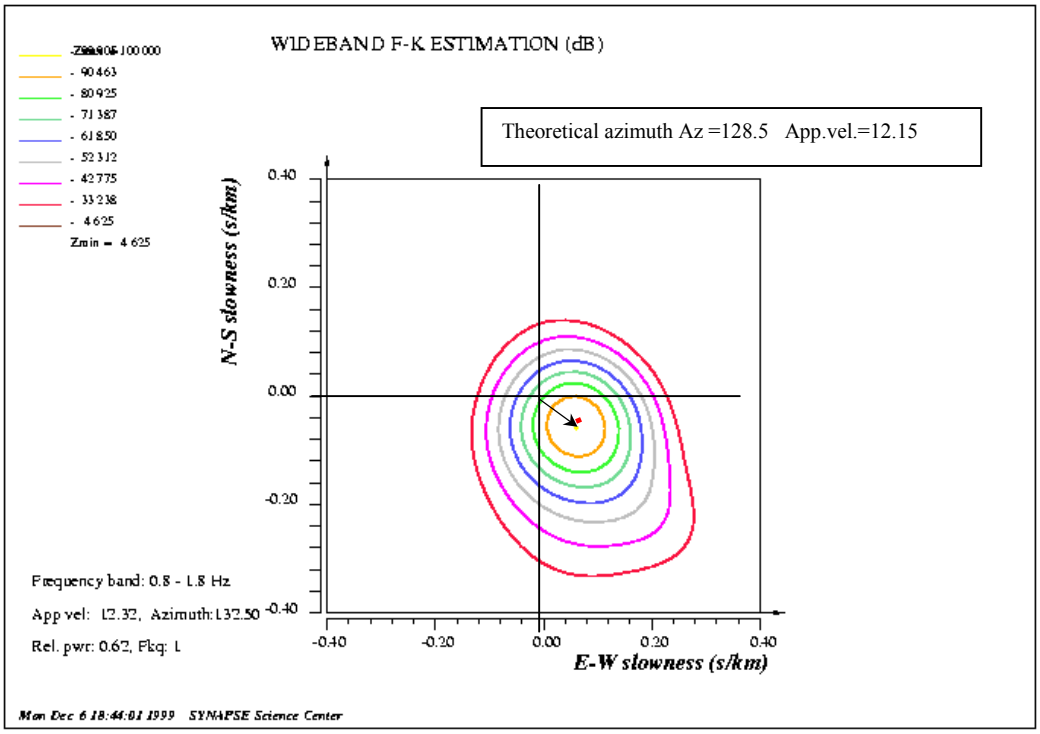

b

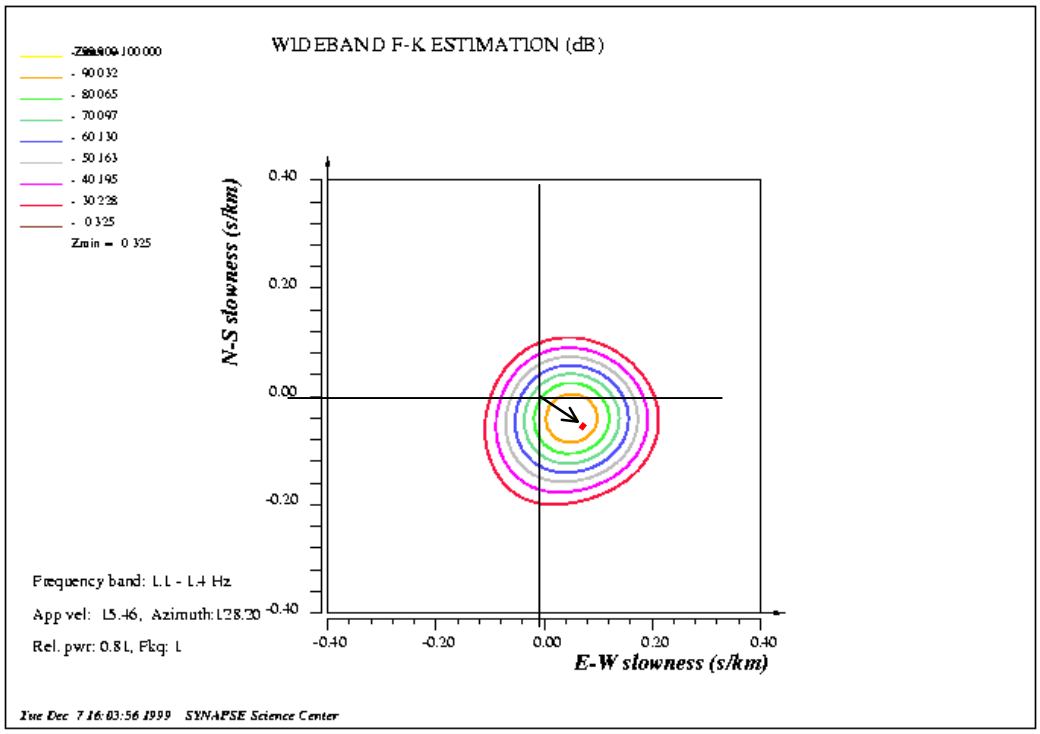

Fig.1. F-K analysis of the GERESS Dead Sea explosion on 99.11.11 by wideband conventional F-K in 0.8-1.8 Hz band (a), and 1.2-1.4 Hz band (b).

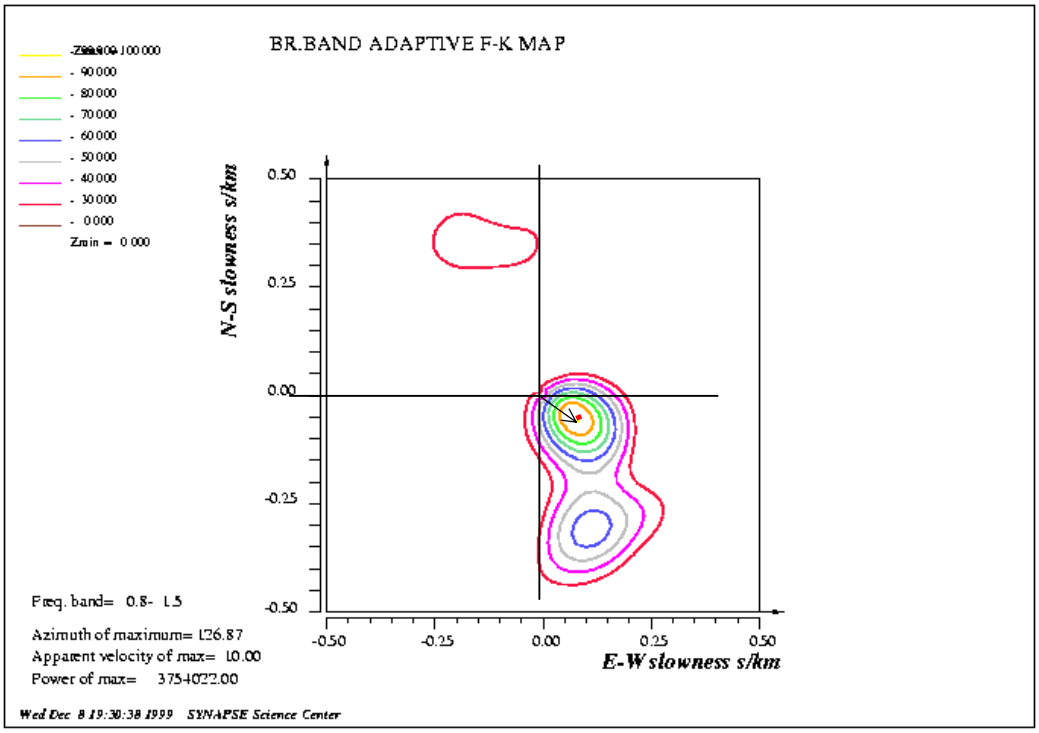

Fig.2. The AF-K slowness analysis of the GERESS Dead Sea explosion on 99.11.11 in 0.8-1.5 Hz band.

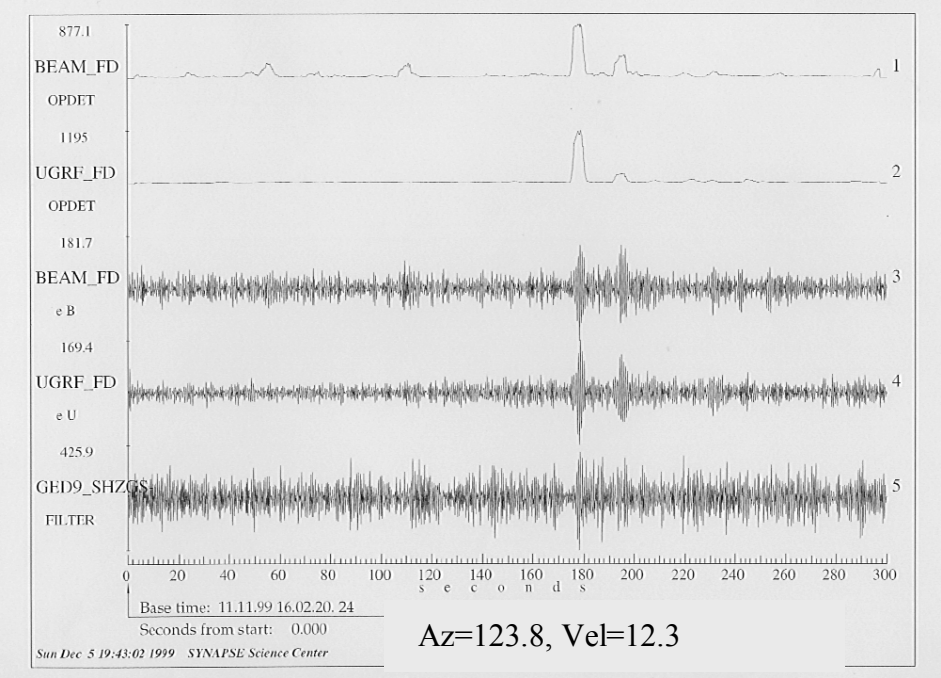

Fig.3. Application of the AOGF to the GERESS Dead Sea explosion recordings. The AOGF (UGRF – Undisturbed GRoup Filter) trace (4) is compared to the beam and GED9 channel recordings in the (1-3 Hz) frequency range. The 1C traces of the Optimal Detector for the beam and UGRF are at the top.

2. Application of the Maximum Likelihood Techniques.

A novel approach for ***M*** dimensional array signal detection and parameter estimation is a Maximum Likelihood Technique of Böhme (1995). The algorithm is destined for recognition of multiple seismic phases arriving to an array with ***m*** different azimuths and apparent velocities, which are distinguished in the procedure by a statistical projection method. The analysis is based on the frequency domain ***SNR(f, t)*** estimation, within time domain moving window. We introduced some simplification of the method resulting in statistics ***FM(t)*** and ***fm(t),*** with directly computed probability distributions, that are theoretically known in the case of white background noise. These statistics are defined as follows:

$$F(f_i,\vec{\xi}_m)=\max_{\xi_1,\ldots,\xi_m} SNR_m(f_i)$$
$$FM(t)=\max_{i=1,\ldots,P} F(f_i,\vec{\xi}_m)$$
$$fm(t)=\min_{i=1,\ldots,P} F(f_i,\vec{\xi}_m) \qquad (2)$$

The probability distributions of the ***FM(t)*** and ***fm(t)*** statistics are defined via the standard ***F*** probability distribution function

$$1-\alpha = P\{FM \le \kappa_m^{\alpha}\} = U(\kappa_m^{\alpha})^P$$
$$1-\beta = P\{fm \le \kappa_{m+1}^{\beta}\} = 1-(1-U(\kappa_{m+1}^{\beta}))^P \qquad (3)$$

where f_i is the i-th FFT frequency $i= 1,\ldots,p$; 2D vector k is slowness, $U=F_{2p,2p(M-m-1)}$ denotes standard Fisher distribution with given degrees of freedom; □, □. – given probabilities of false alarm for each of the statistics: maximum ***FM(t)*** and minimum ***fm(t)*** respectively.

The results of application of the method to the GERESS recordings of the Dead Sea explosion signal is demonstrated in the Table 2 and on Fig. 4 (a, b), showing five subplots: 1) seismogram and theoretical P arrival (arrow), 2) moving window statistics of the ***FM(t)*** and ***fm(t),*** 3) number of the detected sources ***N(t),*** 4)azimuth estimates ***Az(t)*** and 5) apparent velocity ***Vel(t).*** The sequential test with test level α = 0.01is carried out over each seismogram sliding window of 3.2 sec length and of 0.5 sec shift unit. The seismograms are pre-filtered in the several indicated below frequency bands. .

Table 2. Results of MLTM processing of GERESS recordings for the Dead Sea 5 t shot *(distance: 23.84 deg., P-arrival time: 15:05:15.6).*

Estimation	Filter	Azimuth, degree	Apparent Velocity, km/sec
Theory (IASPEI91)	-	128.5	12.14
IDC (Beamforming)	narrow BP	127	10
MLTM algorithm	No filter	135.3	12.7
	0.8-1.8 Hz	132.7	13.3
	0.8-1.5 Hz	137.7	14.5
	1.1-1.4 Hz	129.9	15.4

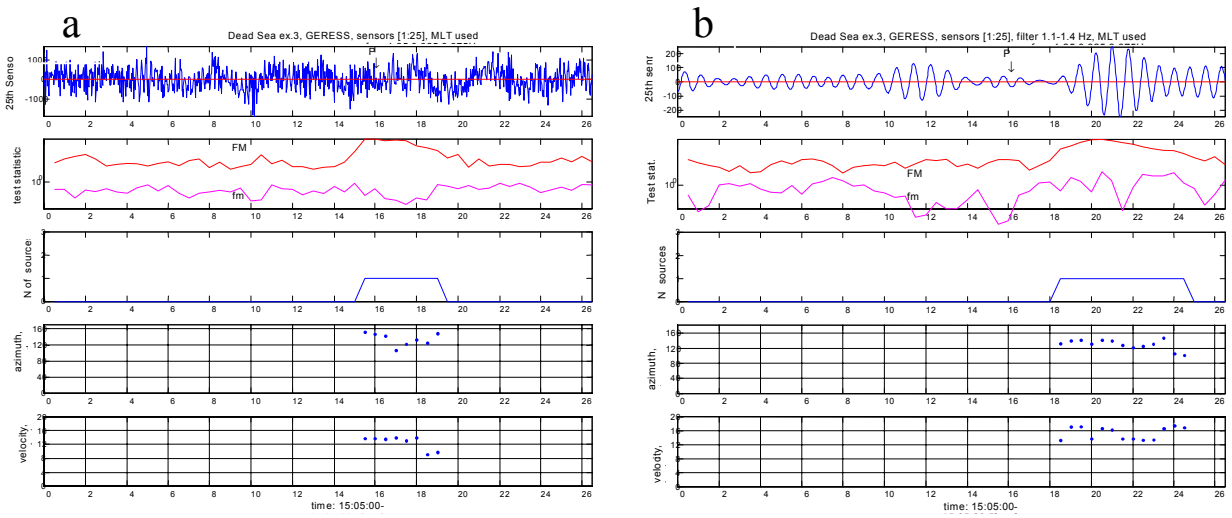

Fig. 4. MLTM processing for the Dead Sea shot with no pre-filtering (a) and BP filtering in 1.1-1.4 Hz (b).

3. Application of the MLTM to the EILESA.

The Eilat Experimental Seismic Array (EILESA), was established in 1998, 15 km to the north of the town of Eilat. It consists of 13 short-period (L4C seismometer) stations, including a reference 3-C station inside the 200 m long tunnel, co-located with the BB station EIL (Fig. 5a.). Eight of the array stations recorded the last of the explosions situated at a. distance of 255 km and azimuth 16^{o} (Fig. 5b). The MLT was applied with 21 even frequency bins in the 1.17-8.98 Hz range. The false alarm rate $\alpha_1 = 0.01$, $\alpha_2 = 0.02$. The moving window length is 128 points (50 Hz sampling rate) shifting by 20 samples for each time bin. The results are demonstrated on Fig.6, which show that there is detection of one source in true P wave arrival time, but the detection lasts continuously 5 sec only. Then it stops possibly due to the destroying of the signal coherency by the scattered waves. The azimuth estimates vary in time beginning from the negative values and decreasing down to –18^{o}. Then they rise up to12^{o}. Probably the effect is due to the wave diffraction caused by a heterogeneity. The apparent velocity estimate, high in the beginning, decreases gradually, and finally reaches the true 6 km/sec level, where it oscillates.

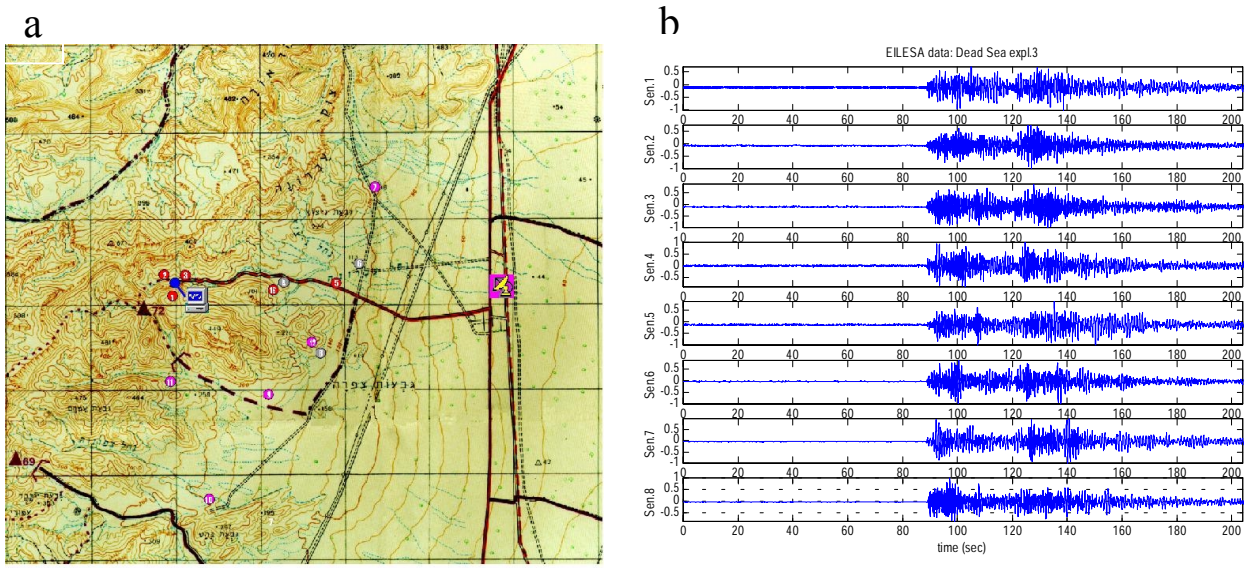

Fig. 5. 13 element EILESA array. Configuration (a), the 5 t Dead Sea explosion recordings at R=255 km and Az=16 ^{o} (b).

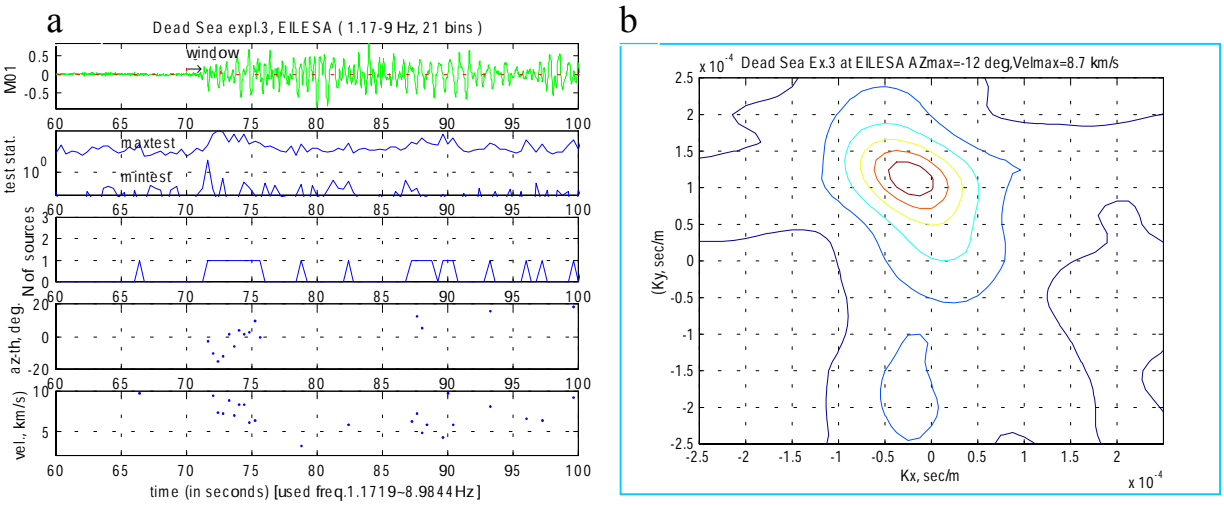

Fig. 6. The Dead Sea explosion record by the EILESA array and the MLTM detection and parameter estimation (a). Values of the FM statistic versus slowness *(Kx, Ky)* for the 72 sec time point (b). The maximum of the statistic corresponds to the Az = -12 ^{o}, Vel = 8.7 km/sec.

4. Evaluation of the travel-time model using the Dead Sea explosions data.

One of the main goals of the Dead Sea experiment is calibration of the IMS and other stations in the area. The true known source location and ignition time provide unique opportunity for measuring exact real travel times. All the explosion's P waves were observable all over the Israel and Jordan seismic networks (ISN and JSN) in the distance range 8 – 240 km and also at Cyprus up to 500 km. We measured P travel times for the three explosions and noticed that for the most of stations they fell in rather small 0.2 sec time interval. The picks were then compared to the travel times (see Fig. 7) corresponding to the two velocity models: the 3-layer and the 4-layer one. The 3-layer model was in use for the ISN location purpose previously (Seismological Bulletin No.11, 1992) (see Table 3), and the 4-layer is the present one (Table 4). For some of the picks there are considerable deviations in the both cases.

Then, we looked for the model better matching our P pickings. The four layer stratified model was chosen from visual inspection of the data and the best fit depths and velocities were obtained by the least-square method according to full-range scanning within given parameter intervals. After that the result was further improved by application of the Levenberg-Markvardt optimization procedure. Most of Jordan stations (see, for example, LISJ,KFNJ, SALJ on Fig. 7.) show delays of ~0.7 sec from the ISN best-fit travel time curve for the reason which is still to be clarified. Probably, this is due to the leap of media properties from one to another side of the Jordan fault or simply, this is due to the watch problems. Thus, the outliers were excluded from the optimization procedure and only matching well N = 80 observations were selected. Final residuals $dt_j=T_{obs,j}-T_{calc,j}$ $,j=1,...N$ have RMS=0.201 sec compared to RMS=0.32 and RMS=0.71 for the two models mentioned above respectively. The notable feature of the best-fit model (Table 5) is a ~1 km thicker layer of the sediments with average Vp=3.77 km/sec, providing relatively large delays of the P waves at the closer stations (< 10 km). The model agrees also to the parameters obtained in the joint hypocenter determination procedure (see Table 6) (Dr. N. Rabinowitz, personal communication).

We tried to examine the travel time dependency on azimuth by computation of the deviations from the best-fit model for the different stations. There is known thickening of the crust in the Southeastern direction, so the azimuth dependant deviation from the best-fit model was expected. Unfortunately, the azimuth coverage is not representative in the East-Western direction and thus the data we have didn't allow us to notice the effect.

Table 3. Velocity model used previously.

Thickness, km	Vp, km/sec	Vs, km/sec
2.1	3.5	2.0
10.6	5.7	3.2
15.5	6.4	3.6
	7.9	4.4

Table 4. Present Velocity model.

Thickness, km	Vp, km/sec	Vs, km/sec
2.56	4.36	2.45
7.2	5.51	3.10
21.64	6.23	3.50
100	7.95	4.46
	8.15	4.60

Table 5. Best-fit velocity model

Thickness, km	Vp, km/sec	Vs, km/sec
3.35	3.77	2.12
3.18	6.00	3.37
12.16	6.11	3.43
13.77	6.73	3.78
	7.88	4.43

Table 6. Joint Epicenter Solution model

Thickness, km	Vp
2	3.03
3	5.60
5	6.21
5	6.39
6	6.61
7	7.05
17	7.61
20	8.10

5. Automatic picking and location of the explosions.

We applied robust automatic locator (Pinsky, 1999), developed in the frame of the contract, to the ISN and JSN recordings of the three events, using the best-fit velocity model. The locator is the two-stage procedure, using envelope location at the first stage to estimate the time intervals for the P, S first arrivals to the network stations. The second stage comprises automatic picking of the P, S first arrivals with robust fitting of the picks (automatically eliminating outliers) to the travel time model. The results of the automatic location are presented in the Table 7 together with true coordinates and manual-picking location results. The latter are due to the conventional velocity model used (Table 4.). The results show accurate location in the automatic case and a somewhat shifting for manual picking due to the conventional model imperfection.

Table 7. Location of the Dead Sea explosions by an analyst and the automatic locator.

Date	Charge, kg	M_L	AXES	GPS, km	Analyst Solution, km	ERROR km	Automatic Locator, km	ERROR, km
08.11.99	500	3.1	X Y H	191.957 104.594 0.5	188.20 105.6 2	-3.76 1.00 2	192.3 103.9 0	0.3 -0.6 -0.5
10.11.99	2000	3.6	X Y H	191.897 104.686 0.5	190.4 104.5 3	1.50 -0.19 3	191.9 104.1 1	0.0 0.6 0.5
11.11.99	5000	3.9	X Y H	192.023 104.661 0.5	191.1 103.7 2	-0.92 0.96 2	192. 104.7 5	0. 0. 4.5

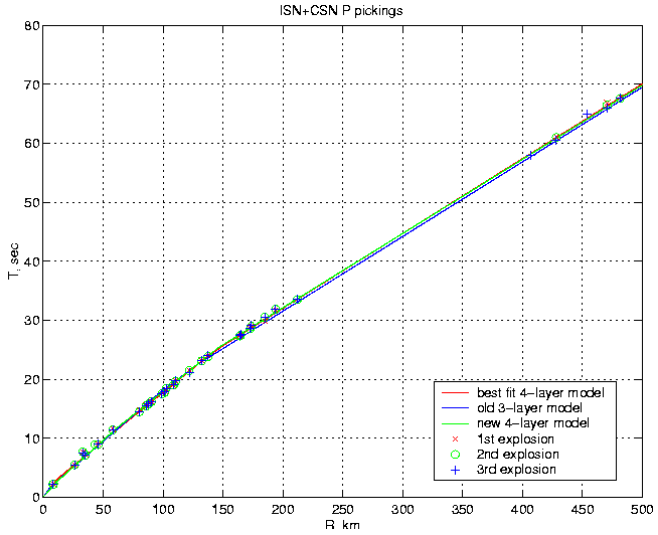

Fig. 7. P travel times for the three stratified models and the P picks for the three explosions.